

Spin multistability in dissipative polariton channelsÖ. Bozat,^{1,2} I. G. Savenko,^{3,4} and I. A. Shelykh^{3,4}¹*International Institute of Physics, Avenida Odilon Gomes de Lima, 1772, Capim Macio, 59078-400, Natal, Brazil*²*Faculty of Engineering and Natural Sciences, Sabancı University, Orhanlı - Tuzla 34956, Istanbul, Turkey*³*Science Institute, University of Iceland, Dunhagi 3, IS-107 Reykjavik, Iceland*⁴*Division of Physics and Applied Physics, Nanyang Technological University, 637371, Singapore*

(Received 4 May 2012; revised manuscript received 4 June 2012; published 10 July 2012)

We present a model for the theoretical description of the dynamics of a system of spinor cavity polaritons in real space and time, accounting for all relevant types of the interactions and effective magnetic fields. We apply our general formalism for the consideration of the polarization dynamics of the coherently driven, one-dimensional polariton channel. We investigate the effect of the temperature and the longitudinal-transverse splitting on the spin (polarization) multistability and hysteresis arising from the polarization-dependent polariton-polariton interaction. We show that the effect of the phase of the driving laser pump is as important as its strength, and demonstrate that the multistability behavior can survive up to high temperatures in the presence of longitudinal-transverse splitting.

DOI: [10.1103/PhysRevB.86.035413](https://doi.org/10.1103/PhysRevB.86.035413)

PACS number(s): 72.25.Dc, 71.36.+c, 72.10.Di, 42.50.Pq

I. INTRODUCTION

Cavity polaritons are composite particles, arising from strong coupling between the photonic mode of a planar semiconductor microcavity and the exciton transition in a quantum well (QW), embedded in the cavity at the point where the electric field of the confined electromagnetic state reaches its maximum. Due to their hybrid half-light-half-matter nature, cavity polaritons demonstrate a set of peculiar properties which make them different from other quasiparticles in solid-state systems. An extremely low effective mass of the cavity polaritons (about 10^{-4} – 10^{-5} of the free electron mass) together with strong polariton-polariton interactions make the polaritonic system an ideal candidate for the observation of the variety of quantum collective phenomena at surprisingly high temperatures. Achievement of polariton Bose-Einstein condensation was first reported at $T = 20$ K (Ref. 1) and later on even at room temperature.² Subsequently, polariton superfluidity,³ the Josephson effect,⁴ and the formation of topological excitations⁵ were experimentally observed. Other theoretically predicted effects such as polariton self-trapping⁶ and polariton-mediated superconductivity⁷ still wait for their experimental confirmation.

Besides fundamental interest, quantum microcavities in the strong-coupling regime can be used for optoelectronic applications.⁸ For more than a decade, the only object of the study in this context was the polariton laser,⁹ a novel type of the coherent emitter which explores the possibility of the polariton BEC. In recent years, however, the emphasis was to shift to other types of the devices based on the transport properties of cavity polaritons in real space. It was noticed that the peculiar spin structure of polaritons opens a way for the creation of optical analogs of spintronic components (so-called spinoptronic devices).¹⁰ With respect to optics, spinoptronics has the advantage of being able to use particle-particle interactions occurring in nanostructures and resulting in strong nonlinearities. With respect to spintronics, it has the advantage of strongly reducing the dramatic impact of carrier spin relaxation or decoherence, which has severely limited the achievement or the functionality of any working semiconductor-based spintronic devices.

In this context, the analysis of one-dimensional (1D) polariton transport is of particular importance,¹¹ as 1D polariton channels are the fundamental building blocks of such future spinoptronic devices as polariton neurons¹² and polariton integrated circuits.¹³ It should be noted that the current state of growth technology offers a large variety of methods of the lateral confinement of cavity polaritons,¹⁴ and polariton quantum wires (1D polariton channels) can be routinely produced.

Currently, the theoretical study of transport of spinor cavity polaritons in real space is based on the assumption of full coherence of the polaritonic system. Polariton-polariton interactions are either neglected^{15–17} or treated within frameworks of spinor Gross-Pitaevskii equations (GPe).¹⁸ The noncoherent processes coming from the interaction of the polaritonic system with a phonon bath in most cases are not accounted for or treated within simple phenomenological models lacking microscopic justification.^{19–21} On the other hand, it is clear that polariton-phonon interaction is of crucial importance, as it provides a thermalization mechanism in a polaritonic ensemble^{22,23} and can affect such experimentally observable quantities as first- and second-order coherencies.^{24,25} Note in this context that there are also other effects which influence the coherence functions, for instance particle-number fluctuations together with the interparticle interactions.²⁶

It should be noted that for a spatially homogeneous polariton system, polariton-phonon interactions can be accounted for using a system of the semiclassical Boltzmann equations.^{27–30} This method, however, has several serious drawbacks. First, it is based on the assumption that the system is fully incoherent, and thus a variety of intriguing nonlinear phenomena such as bistability and multistability cannot be described. Second, it provides the information about occupation numbers in the reciprocal space only, and thus cannot be used for a description of the dynamics of the spatially inhomogeneous system. This makes this formalism inappropriate for the modeling of spinoptronic devices based on polariton transport in real space.

In the present paper, we present formalism suitable for the description of the dynamics of an inhomogeneous spinor polariton system in real space and time, accounting for all relevant types of processes. Namely, we take into account

polariton-polariton and polariton-phonon interactions and an effective longitudinal-transverse (TE-TM) magnetic field acting on polariton spin. Our consideration is based on the Lindblad approach for density matrix dynamics and represents a generalization of our previous work where the spinless case was considered.^{31,32} We use our results for modeling the spin dynamics of the polaritons in 1D channels, investigating the role played by decoherence at different temperatures.

II. FORMALISM

We describe the state of the system (polaritons plus phonons) by its density matrix χ , for which we apply the Born approximation factorizing it into the phonon part, which is supposed to be time independent and corresponds to the thermal distribution of acoustic phonons $\chi_{ph} = \exp\{-\frac{\mathcal{H}_{ph}}{k_B T}\}$ and the polariton part χ_{pol} whose time dependence should be determined, $\chi = \chi_{ph} \otimes \chi_{pol}$. Physically, the application of the Born approximation means that polariton-phonon interaction is relatively weak and no hybrid polariton-phonon modes can be formed. Our aim is to find dynamic equations for the time evolution of the single-particle polariton density matrix in real space and time,

$$\begin{aligned} \rho_{\sigma,\sigma'}(\mathbf{r},\mathbf{r}',t) &= \text{Tr}\{\widehat{\psi}_\sigma^\dagger(\mathbf{r},t)\widehat{\psi}_{\sigma'}(\mathbf{r}',t)\chi\} \\ &= \langle \widehat{\psi}_\sigma^\dagger(\mathbf{r},t)\widehat{\psi}_{\sigma'}(\mathbf{r}',t) \rangle, \end{aligned} \quad (1)$$

where $\widehat{\psi}_\sigma^\dagger(\mathbf{r},t), \widehat{\psi}_{\sigma'}(\mathbf{r},t)$ are operators of the spinor polariton field, the subscripts $\sigma, \sigma' = \pm 1$ denote the z projection of the spin of the cavity polaritons and correspond to right- and left-circular polarized states, and the trace is performed by all the degrees of freedom of the system. The particularly interesting quantities are matrix elements with $\mathbf{r} = \mathbf{r}'$, which give the density and polarization of the polariton field in real space and time,

$$n(\mathbf{r},t) = \sum_{\sigma=\pm 1} \rho_{\sigma,\sigma}(\mathbf{r},\mathbf{r},t), \quad (2)$$

$$S_z(\mathbf{r},t) = \frac{1}{2}[\rho_{+1,+1}(\mathbf{r},\mathbf{r},t) - \rho_{-1,-1}(\mathbf{r},\mathbf{r},t)], \quad (3)$$

$$S_x(\mathbf{r},t) + iS_y(\mathbf{r},t) = \rho_{+1,-1}(\mathbf{r},\mathbf{r},t). \quad (4)$$

The pseudospin vector $\mathbf{S} = (S_x, S_y, S_z)$ describes the polarization of the cavity polaritons. Orientation of the pseudospin along z -axis corresponds to the circular polarization, while the in-plane components S_x, S_y correspond to the linear polarized components.

The off-diagonal matrix elements with $\mathbf{r} \neq \mathbf{r}'$ also have physical meaning and describe spatial coherence in the system.

To obtain expressions for the temporal dynamics of the components of a single-particle density matrix, it is convenient to go to the reciprocal space, making a Fourier transform of the single particle density matrix,

$$\begin{aligned} \rho_{\sigma,\sigma'}(\mathbf{k},\mathbf{k}',t) &= (2\pi)^d/L^d \int e^{i(\mathbf{k}\mathbf{r}-\mathbf{k}'\mathbf{r}')} \rho_{\sigma,\sigma'}(\mathbf{r},\mathbf{r}',t) d\mathbf{r}d\mathbf{r}' \\ &= \text{Tr}\{a_{\sigma,\mathbf{k}}^+ a_{\sigma',\mathbf{k}'} \chi\} \equiv \langle a_{\sigma,\mathbf{k}}^+ a_{\sigma',\mathbf{k}'} \rangle, \end{aligned} \quad (5)$$

where d is the dimensionality of the system ($d = 2$ for nonconfined polaritons, $d = 1$ for the polariton channel), L is its linear size, and $a_{\sigma\mathbf{k}}^+, a_{\sigma\mathbf{k}}$ are the creation and annihilation operators of the polaritons, respectively, with circular polarization σ and momentum \mathbf{k} . Note that we have chosen the prefactor in a Fourier transform in such a way that the values of $\rho(\mathbf{k},\mathbf{k}',t)$ are dimensionless, and diagonal matrix elements give occupation numbers of the states in discretized reciprocal space. Knowing the density matrix in reciprocal space, we can find the density matrix in real space by applying the inverse Fourier transform.

The total Hamiltonian of the system can be represented as a sum of two parts,

$$\mathcal{H} = \mathcal{H}_1 + \mathcal{H}_2, \quad (6)$$

where the first term \mathcal{H}_1 describes the ‘‘coherent’’ part of the evolution, corresponding to free polariton propagation, polariton-polariton interactions, and the effect of TE-TM splitting, and the second term \mathcal{H}_2 corresponds to the dissipative interaction with acoustic phonons. The two terms affect the polariton density matrix in a qualitatively different way.

A. Polariton-polariton interactions

The part of the evolution corresponding to \mathcal{H}_1 is given by the following expression:

$$\begin{aligned} \mathcal{H}_1 &= \sum_{\mathbf{k}\sigma} E_{\mathbf{k}} a_{\mathbf{k}\sigma}^+ a_{\mathbf{k}\sigma} + \sum_{\mathbf{k},\sigma} \Omega(\mathbf{k}) a_{\mathbf{k},\sigma}^+ a_{\mathbf{k},-\sigma} \\ &+ U_1 \sum_{\mathbf{k}_1,\mathbf{k}_2,\mathbf{p},\sigma} a_{\mathbf{k}_1,\sigma}^+ a_{\mathbf{k}_2,\sigma}^+ a_{\mathbf{k}_1+\mathbf{p},\sigma} a_{\mathbf{k}_2-\mathbf{p},\sigma} \\ &+ U_2 \sum_{\mathbf{k}_1,\mathbf{k}_2,\mathbf{p},\sigma} a_{\mathbf{k}_1,\sigma}^+ a_{\mathbf{k}_2,-\sigma}^+ a_{\mathbf{k}_1+\mathbf{p},\sigma} a_{\mathbf{k}_2-\mathbf{p},-\sigma}, \end{aligned} \quad (7)$$

where $E_{\mathbf{k}}$ gives the dispersion of the polaritons, $\Omega(\mathbf{k})$ is the TE-TM splitting corresponding to the in-plane effective magnetic field leading to the rotation of the pseudospin of cavity polaritons, U_1 is the matrix element of the interaction between polaritons of the same circular polarization, and U_2 is the matrix element of the interaction between polaritons of opposite circular polarizations. In the current paper, we neglect for simplicity the \mathbf{p} dependence of the polariton-polariton interaction constant coming from Hopfield coefficients. As well, we will suppose $\Omega(\mathbf{k}) = \text{const}$, which corresponds well to the situation of the polariton channel (but not for a 2D polariton system).

The effect of \mathcal{H}_1 on the evolution of the density matrix is described by the Liouville-von Neumann equation,

$$i\hbar(\partial_t \chi)^{(1)} = [\mathcal{H}_1; \chi], \quad (8)$$

which after the use of the mean-field approximation leads to the following dynamic equations for the elements of the single-particle density matrix in the reciprocal space (the derivation

is completely analogical to those presented in Ref. 31):

$$\begin{aligned}
 -i\hbar\{\partial_t\rho_{\sigma,\sigma'}(\mathbf{k},\mathbf{k}')\}^{(1)} &= (E_{\mathbf{k}} - E_{\mathbf{k}'})\rho_{\sigma,\sigma'}(\mathbf{k},\mathbf{k}') + \Omega[\rho_{-\sigma,\sigma'}(\mathbf{k},\mathbf{k}') - \rho_{\sigma,-\sigma'}(\mathbf{k},\mathbf{k}')] \\
 &+ U_1 \sum_{\mathbf{k}_1,\mathbf{p}} [\rho_{\sigma,\sigma}(\mathbf{k}_1,\mathbf{k}_1 - \mathbf{p})\rho_{\sigma,\sigma'}(\mathbf{k} - \mathbf{p},\mathbf{k}'), -\rho_{\sigma',\sigma'}(\mathbf{k}_1,\mathbf{k}_1 - \mathbf{p})\rho_{\sigma,\sigma'}(\mathbf{k},\mathbf{k}' + \mathbf{p})] \\
 &+ U_2 \sum_{\mathbf{k}_1,\mathbf{p}} [\rho_{-\sigma,-\sigma}(\mathbf{k}_1,\mathbf{k}_1 - \mathbf{p})\rho_{\sigma,\sigma'}(\mathbf{k} - \mathbf{p},\mathbf{k}') - \rho_{-\sigma',-\sigma'}(\mathbf{k}_1,\mathbf{k}_1 - \mathbf{p})\rho_{\sigma,\sigma'}(\mathbf{k},\mathbf{k}' + \mathbf{p})]. \quad (9)
 \end{aligned}$$

B. Scattering with acoustic phonons

Polariton-phonon scattering corresponds to the interaction of the quantum polariton system with the classical phonon reservoir. It is of a dissipative nature, and thus the straightforward application of the Liouville-von Neumann equation is impossible. One should rather use the approach based on the Lindblad formalism, which is standard in quantum optics and results in the master equation for the full density matrix of the system.³³ For the convenience of the reader, we give the main steps of the derivation of the dissipative part of dynamic equations for a spinor polariton system, omitting, however, all of the technical details, which can be found elsewhere.³¹

The Hamiltonian of the interaction of polaritons with acoustic phonons in the Dirac picture can be represented as

$$\begin{aligned}
 \mathcal{H}_2(t) &= \mathcal{H}^-(t) + \mathcal{H}^+(t) \\
 &= \sum_{\sigma,\mathbf{k},\mathbf{q}} D(\mathbf{q}) e^{i(E_{\mathbf{k}+\mathbf{q}} - E_{\mathbf{k}})t} a_{\sigma,\mathbf{k}+\mathbf{q}}^+ a_{\sigma,\mathbf{k}} (b_{\mathbf{q}} e^{-i\omega_{\mathbf{q}}t} + b_{-\mathbf{q}}^+ e^{i\omega_{\mathbf{q}}t}), \quad (10)
 \end{aligned}$$

where $a_{\sigma\mathbf{k}}$ are operators for spinor polaritons, $b_{\mathbf{q}}$ are operators for spinless phonons, $E_{\mathbf{k}}$ and $\omega_{\mathbf{q}}$ are dispersion relations for polaritons and acoustic phonons, respectively, and $D(\mathbf{q})$ is the polariton-phonon coupling constant. In the last equality, we separated the terms \mathcal{H}^+ where a phonon is created, containing the operators b^+ , from the terms \mathcal{H}^- in which it is destroyed, containing operators b .

Now, one can consider a hypothetical situation when polariton-polariton interactions are absent, and the redistribution of the polaritons in reciprocal space is due to the scattering with acoustic phonons only. One can rewrite the Liouville-von Neumann equation in an integro-differential form and apply the so-called Markovian approximation, corresponding to the situation of fast phase memory loss (see Ref. 33 for the details and discussion of the limits of validity of the approximation),

$$\begin{aligned}
 (\partial_t \chi)^{(2)} &= -\frac{1}{\hbar^2} \int_{-\infty}^t dt' [\mathcal{H}_2(t); [\mathcal{H}_2(t'); \chi(t)]] \\
 &= \delta_{\Delta E} [2(\mathcal{H}^+ \chi \mathcal{H}^- + \mathcal{H}^- \chi \mathcal{H}^+) \\
 &\quad - (\mathcal{H}^+ \mathcal{H}^- + \mathcal{H}^- \mathcal{H}^+) \chi - \chi (\mathcal{H}^+ \mathcal{H}^- + \mathcal{H}^- \mathcal{H}^+)], \quad (11)
 \end{aligned}$$

where the coefficient $\delta_{\Delta E}$ denotes energy conservation and has dimensionality of inverse energy, and in the calculation is taken to be equal to the broadening of the polariton state.³⁴ For the time evolution of the mean value of any arbitrary operator $\langle \hat{A} \rangle = \text{Tr}(\chi \hat{A})$ due to scattering with phonons, one thus has (the derivation of this formula is represented in Ref. 31)

$$\{\partial_t \langle \hat{A} \rangle\}^{(2)} = \delta_{\Delta E} (\langle [\mathcal{H}^-; [\hat{A}; \mathcal{H}^+]] \rangle + \langle [\mathcal{H}^+; [\hat{A}; \mathcal{H}^-]] \rangle). \quad (12)$$

Putting $\hat{A} = a_{\sigma,\mathbf{k}}^+ a_{\sigma',\mathbf{k}'}$ in this equation, we get the contributions to the dynamic equations for the elements of the single-particle density matrix coming from polariton-phonon interaction:

$$\begin{aligned}
 \{\partial_t n_{\mathbf{k},\sigma}\}^{(2)} &= \sum_{\mathbf{q}, E_{\mathbf{k}} < E_{\mathbf{k}+\mathbf{q}}} 2W(\mathbf{q}) \left\{ (n_{\mathbf{k},\sigma} + 1)n_{\mathbf{k}+\mathbf{q},\sigma} (n_{\mathbf{q}}^{ph} + 1) - n_{\mathbf{k},\sigma} (n_{\mathbf{k}+\mathbf{q},\sigma} + 1)n_{\mathbf{q}}^{ph} \right. \\
 &\quad \left. + \frac{1}{2} [\rho_{\sigma,-\sigma}(\mathbf{k},\mathbf{k})\rho_{-\sigma,\sigma}(\mathbf{k} + \mathbf{q},\mathbf{k} + \mathbf{q}) + \rho_{-\sigma,\sigma}(\mathbf{k},\mathbf{k})\rho_{\sigma,-\sigma}(\mathbf{k} + \mathbf{q},\mathbf{k} + \mathbf{q})] \right\} \\
 &+ \sum_{\mathbf{q}, E_{\mathbf{k}} > E_{\mathbf{k}+\mathbf{q}}} 2W(\mathbf{q}) \left\{ (n_{\mathbf{k},\sigma} + 1)n_{\mathbf{k}+\mathbf{q},\sigma} n_{-\mathbf{q}}^{ph} - n_{\mathbf{k},\sigma} (n_{\mathbf{k}+\mathbf{q},\sigma} + 1)(n_{-\mathbf{q}}^{ph} + 1) \right. \\
 &\quad \left. - \frac{1}{2} [\rho_{\sigma,-\sigma}(\mathbf{k},\mathbf{k})\rho_{-\sigma,\sigma}(\mathbf{k} + \mathbf{q},\mathbf{k} + \mathbf{q}) + \rho_{-\sigma,\sigma}(\mathbf{k},\mathbf{k})\rho_{\sigma,-\sigma}(\mathbf{k} + \mathbf{q},\mathbf{k} + \mathbf{q})] \right\}, \quad (13)
 \end{aligned}$$

$$\begin{aligned}
 \{\partial_t \rho_{\sigma,-\sigma}(\mathbf{k},\mathbf{k})\}^{(2)} &= \sum_{\mathbf{q}, E_{\mathbf{k}} < E_{\mathbf{k}+\mathbf{q}}} 2W(\mathbf{q}) \left\{ [\rho_{\sigma,-\sigma}(\mathbf{k},\mathbf{k}) \left[\frac{1}{2}(n_{\mathbf{k}+\mathbf{q},\sigma} + n_{\mathbf{k}+\mathbf{q},\sigma'} - n_{\mathbf{q}}^{ph}) \right] + \rho_{\sigma,-\sigma}(\mathbf{k} + \mathbf{q},\mathbf{k} + \mathbf{q}) \left[\frac{1}{2}(n_{\mathbf{k},\sigma} + n_{\mathbf{k},\sigma'}) + n_{\mathbf{q}}^{ph} + 1 \right] \right\} \\
 &- \sum_{\mathbf{q}, E_{\mathbf{k}} > E_{\mathbf{k}+\mathbf{q}}} 2W(\mathbf{q}) \left\{ \rho_{\sigma,-\sigma}(\mathbf{k},\mathbf{k}) \left[\frac{1}{2}(n_{\mathbf{k}+\mathbf{q},\sigma} + n_{\mathbf{k}+\mathbf{q},\sigma'}) + n_{-\mathbf{q}}^{ph} + 1 \right] + \rho_{\sigma,-\sigma}(\mathbf{k} + \mathbf{q},\mathbf{k} + \mathbf{q}) \left[\frac{1}{2}(n_{\mathbf{k},\sigma} + n_{\mathbf{k},\sigma'}) - n_{-\mathbf{q}}^{ph} \right] \right\}, \quad (14) \\
 \{\partial_t \rho_{\sigma,\sigma}(\mathbf{k},\mathbf{k}')\}^{(2)} &= \sum_{\mathbf{q}, E_{\mathbf{k}} < E_{\mathbf{k}+\mathbf{q}}} W(\mathbf{q}) [\rho_{\sigma,\sigma}(\mathbf{k},\mathbf{k}') (n_{\mathbf{k}+\mathbf{q},\sigma} - n_{\mathbf{q}}^{ph}) + \rho_{-\sigma,\sigma}(\mathbf{k},\mathbf{k}') \rho_{\sigma,-\sigma}(\mathbf{k} + \mathbf{q},\mathbf{k} + \mathbf{q})] \\
 &- \sum_{\mathbf{q}, E_{\mathbf{k}} > E_{\mathbf{k}+\mathbf{q}}} W(\mathbf{q}) [\rho_{\sigma,\sigma}(\mathbf{k},\mathbf{k}') (n_{\mathbf{k}+\mathbf{q},\sigma} + n_{\mathbf{q}}^{ph} + 1) + \rho_{-\sigma,\sigma}(\mathbf{k},\mathbf{k}') \rho_{\sigma,-\sigma}(\mathbf{k} + \mathbf{q},\mathbf{k} + \mathbf{q})]
 \end{aligned}$$

$$\begin{aligned}
 & + \sum_{\mathbf{q}, E_{\mathbf{k}'} < E_{\mathbf{k}'+\mathbf{q}}} W(\mathbf{q}) [\rho_{\sigma, \sigma}(\mathbf{k}, \mathbf{k}') (n_{\mathbf{k}'+\mathbf{q}, \sigma} - n_{\mathbf{q}}^{ph}) + \rho_{\sigma, -\sigma}(\mathbf{k}, \mathbf{k}') \rho_{-\sigma, \sigma}(\mathbf{k}' + \mathbf{q}, \mathbf{k}' + \mathbf{q})] \\
 & - \sum_{\mathbf{q}, E_{\mathbf{k}'} > E_{\mathbf{k}'+\mathbf{q}}} W(\mathbf{q}) [\rho_{\sigma, \sigma}(\mathbf{k}, \mathbf{k}') (n_{\mathbf{k}'+\mathbf{q}, \sigma} + n_{\mathbf{q}}^{ph} + 1) + \rho_{\sigma, -\sigma}(\mathbf{k}, \mathbf{k}') \rho_{-\sigma, \sigma}(\mathbf{k}' + \mathbf{q}, \mathbf{k}' + \mathbf{q})], \quad (15)
 \end{aligned}$$

$$\begin{aligned}
 \{\partial_t \rho_{\sigma, -\sigma}(\mathbf{k}, \mathbf{k}')\}^{(2)} = & \sum_{\mathbf{q}, E_{\mathbf{k}} < E_{\mathbf{k}+\mathbf{q}}} W(\mathbf{q}) [\rho_{\sigma, -\sigma}(\mathbf{k}, \mathbf{k}') (n_{\mathbf{k}+\mathbf{q}, \sigma} - n_{\mathbf{q}}^{ph}) + \rho_{-\sigma, -\sigma}(\mathbf{k}, \mathbf{k}') \rho_{\sigma, -\sigma}(\mathbf{k} + \mathbf{q}, \mathbf{k} + \mathbf{q})] \\
 & - \sum_{\mathbf{q}, E_{\mathbf{k}} > E_{\mathbf{k}+\mathbf{q}}} W(\mathbf{q}) [\rho_{\sigma, -\sigma}(\mathbf{k}, \mathbf{k}') (n_{\mathbf{k}+\mathbf{q}, \sigma} + n_{\mathbf{q}}^{ph} + 1) + \rho_{-\sigma, -\sigma}(\mathbf{k}, \mathbf{k}') \rho_{\sigma, -\sigma}(\mathbf{k} + \mathbf{q}, \mathbf{k} + \mathbf{q})] \\
 & + \sum_{\mathbf{q}, E_{\mathbf{k}'} < E_{\mathbf{k}'+\mathbf{q}}} W(\mathbf{q}) [\rho_{\sigma, -\sigma}(\mathbf{k}, \mathbf{k}') (n_{\mathbf{k}'+\mathbf{q}, \sigma'} - n_{\mathbf{q}}^{ph}) + \rho_{\sigma, \sigma}(\mathbf{k}, \mathbf{k}') \rho_{\sigma, -\sigma}(\mathbf{k}' + \mathbf{q}, \mathbf{k}' + \mathbf{q})] \\
 & - \sum_{\mathbf{q}, E_{\mathbf{k}'} > E_{\mathbf{k}'+\mathbf{q}}} W(\mathbf{q}) [\rho_{\sigma, -\sigma}(\mathbf{k}, \mathbf{k}') (n_{\mathbf{k}'+\mathbf{q}, \sigma'} + n_{\mathbf{q}}^{ph} + 1) + \rho_{\sigma, \sigma}(\mathbf{k}, \mathbf{k}') \rho_{\sigma, -\sigma}(\mathbf{k}' + \mathbf{q}, \mathbf{k}' + \mathbf{q})], \quad (16)
 \end{aligned}$$

where $n_{\mathbf{k}, \sigma} = \rho_{\sigma, \sigma}(\mathbf{k}, \mathbf{k})$, $\rho_{+1; -1}(\mathbf{k}) = s_x(\mathbf{k}) + i s_y(\mathbf{k})$, and $W(\mathbf{q})$ denote spin-independent scattering rates with acoustic phonons (see Ref. 31 for the details). The first two equations corresponding to $\mathbf{k} = \mathbf{k}'$ are nothing but the spinor Boltzmann equations for polariton-phonon scattering describing the redistribution of the polaritons in the reciprocal space, which were obtained earlier using other techniques.³⁵ The equations for off-diagonal matrix elements with $\mathbf{k} \neq \mathbf{k}'$ describe their decay, which physically corresponds to the decay of the coherence in the system coming from polariton-phonon interactions. This process strongly depends on the temperature of the system and leads to the transition from coherent to dissipative dynamics, as demonstrated in Ref. 31. In the regime of coherent pump, it is responsible for the disappearance of polarization multistability with the increase of temperature, as is shown below.

C. Pumping terms

In this paper, we concentrate on the case when a system is pumped by an external coherent laser beam. The corresponding

Hamiltonian can be introduced as

$$\mathcal{H}_{cp} = \sum_{\mathbf{k}, \sigma} p_{\mathbf{k}, \sigma}(t) a_{\mathbf{k}, \sigma}^+ + \text{H.c.} \quad (17)$$

Here, $p_{\mathbf{k}}$ is the Fourier transform of the pumping amplitude in real space,

$$p_{\sigma}(\mathbf{x}, t) = P_{\sigma}(\mathbf{x}) e^{i\mathbf{k}_p \mathbf{x}} e^{-i\omega_p t}, \quad (18)$$

where $P_{\sigma}(\mathbf{x})$ is the pumping spot profile in real space, \mathbf{k}_p is an in-plane pumping vector resulting from the inclination of the laser beam with respect to the vertical, and ω_p is the pumping frequency of the single-mode laser. Time evolution of the arbitrary element of density matrix is given by³²

$$\{\partial_t \rho_{\sigma, \sigma'}(\mathbf{k}, \mathbf{k}')\}^{(cp)} = \frac{i}{\hbar} [p_{\mathbf{k}, \sigma}^*(t) \langle a_{\mathbf{k}', \sigma'} \rangle - p_{\mathbf{k}', \sigma'}(t) \langle a_{\mathbf{k}, \sigma} \rangle^*], \quad (19)$$

where the time evolution of the mean values of the annihilation operator reads

$$\begin{aligned}
 \partial_t \langle a_{\mathbf{k}, \sigma} \rangle = & -\frac{i}{\hbar} p_{\mathbf{k}, \sigma}(t) - \frac{i}{\hbar} E_{\mathbf{k}} \langle a_{\mathbf{k}, \sigma} \rangle - \frac{i}{\hbar} \Omega_{\mathbf{k}} \langle a_{\mathbf{k}, -\sigma} \rangle - \frac{i}{\hbar} \sum_{\mathbf{k}_2, \mathbf{p}} [U_1 \rho_{\sigma, \sigma}(\mathbf{k}_2, \mathbf{k}_2 - \mathbf{p}) + U_2 \rho_{-\sigma, -\sigma}(\mathbf{k}_2, \mathbf{k}_2 - \mathbf{p})] \langle a_{\mathbf{k}+\mathbf{p}, \sigma} \rangle \\
 & + \sum_{\mathbf{q}, E_{\mathbf{k}} < E_{\mathbf{k}+\mathbf{q}}} W(\mathbf{q}) [(n_{\mathbf{k}+\mathbf{q}, \sigma} - n_{\mathbf{q}}^{ph}) \langle a_{\mathbf{k}, \sigma} \rangle + \rho_{-\sigma, \sigma}(\mathbf{k} + \mathbf{q}, \mathbf{k} + \mathbf{q}) \langle a_{\mathbf{k}, -\sigma} \rangle] \\
 & - \sum_{\mathbf{q}, E_{\mathbf{k}} > E_{\mathbf{k}+\mathbf{q}}} W(\mathbf{q}) [(n_{\mathbf{k}+\mathbf{q}, \sigma} + n_{\mathbf{q}}^{ph} + 1) \langle a_{\mathbf{k}, \sigma} \rangle + \rho_{-\sigma, \sigma}(\mathbf{k} + \mathbf{q}, \mathbf{k} + \mathbf{q}) \langle a_{\mathbf{k}, -\sigma} \rangle]. \quad (20)
 \end{aligned}$$

D. Dynamics of the polarization

The dynamics of the circular polarization degree \wp_c of the light emission from the ground $k = 0$ state can be defined as

$$\wp_c = \frac{n_{\mathbf{k}=0}^+ - n_{\mathbf{k}=0}^-}{n_{\mathbf{k}=0}^+ + n_{\mathbf{k}=0}^-}, \quad (21)$$

where $n_{\mathbf{k}=0}^+(t)$ and $n_{\mathbf{k}=0}^-(t)$ stand for the populations of polaritons with pseudospin ± 1 correspondingly in the ground state of the dispersion.

One should mention the effect of longitudinal-transverse splitting Ω on the polarization degree dynamics, since it couples the σ^+ and σ^- modes together. Its role becomes more evident if one switches to the pseudospin formalism, which is described in Sec. I. From the formal point of view, TE-TM splitting is equivalent to the effective magnetic field in the $+x$ direction, $\Omega = \mathbf{e}_x \Omega$ (along the quantum wire). At the same time, the polariton-polariton interaction gives rise to another effective magnetic field oriented in the z direction (structure growth axes), $\Omega_{p-p} \propto \mathbf{e}_z (U_1 - U_2) (n^+ - n^-)$ (see Ref. 36). Therefore, the total effective magnetic field

represents superposition $\mathbf{\Omega}_{\text{tot}} = \mathbf{\Omega}_{p-p} + \mathbf{\Omega}$. Accordingly, it is possible to rewrite the kinetic equations as coupled equations for occupation number n_{σ} and in-plane pseudospin \mathbf{S}_{\perp} .⁴¹ Considering only the effect of effective magnetic fields (assuming an infinite lifetime and the absence of interaction with phonons), coupled equations for the pseudospin precession are given as

$$\partial_t n_{\mathbf{k}=0}^+ \propto \mathbf{e}_z \cdot (\mathbf{S}_{\perp} \times \mathbf{\Omega}), \quad (22)$$

$$\partial_t \mathbf{S}_{\perp} \propto (\mathbf{S}_{\perp} \times \mathbf{\Omega}_{p-p}) + \frac{1}{2}(n_{\mathbf{k}=0}^+ - n_{\mathbf{k}=0}^-)\mathbf{\Omega}. \quad (23)$$

This corresponds to the precession of the pseudospin along the time-dependent magnetic field, which leads to its nontrivial dynamics.

III. RESULTS AND DISCUSSION

We consider a microcavity based on the AlGaAs family of alloys and use the following parameters. The Rabi splitting was taken equal to 15 meV, polariton effective mass of 3×10^{-4} of the free electron mass, and detuning between the pure photonic and excitonic modes of 3 meV. The polaritonic quantum wire is $50 \mu\text{m}$ long and $2 \mu\text{m}$ wide. Further, we use the typical polariton lifetime in a medium Q factor microcavity, $\tau = 2$ ps. The polariton-polariton and polariton-phonon scattering rates have been taken independent of the wave vector for simplicity. The matrix element of the polariton-polariton interaction was estimated using the expression $U \approx 3E_b a_B^2/A$, where E_b is the exciton binding energy, a_B is its Bohr radius, and A is the area of the wire, which gives $U \approx 20$ neV. The polariton-phonon scattering rate $W = 10^8 \text{ s}^{-1}$. The pump laser is detuned above the energy of the lower polariton branch by $\delta = 1$ meV. We consider the case of a spatially homogeneous cw pump of different polarizations.

The bistable (for spinless condensate) and multistable (if one accounts for the spin) behavior of a polariton system in 1D and 2D quantum systems has already been investigated theoretically in a number of works (see, for instance, Ref. 37) and was reported experimentally.^{38–40} Most of the theoretical approaches are based on the solution of the GPe. Unfortunately, this technique does not allow one to account for the dissipation dynamics of polaritons due to interaction with the crystal lattice (phonon-mediated processes). The density matrix approach, which is being developed in the current paper, does. In the limiting case of zero temperature, we immediately reproduce the results obtained by the GPe, as expected.

The multistability (with multihysteresis) characteristic is shown in Fig. 2 for different temperatures in the range 1–100 K, in the absence of TE-TM splitting. In this case, since there is no mechanism of the transition between the σ^+ and σ^- modes, this effect can be understood in terms of the independent bistable dynamics of the σ^+ and σ^- modes. Accordingly, in the inset, we present the population hysteresis curve of spinless polaritons to clarify the forthcoming discussion. Let us begin with the inset. In the certain range of pumps, the polariton population can take two different values depending on the history of the pumping process. If we slowly increase the intensity of the pump, at some threshold value $P_{th}^{(\rightarrow)}$ the population of the ground state jumps up abruptly due to the resonance of the blue shifted polariton energy with the energy

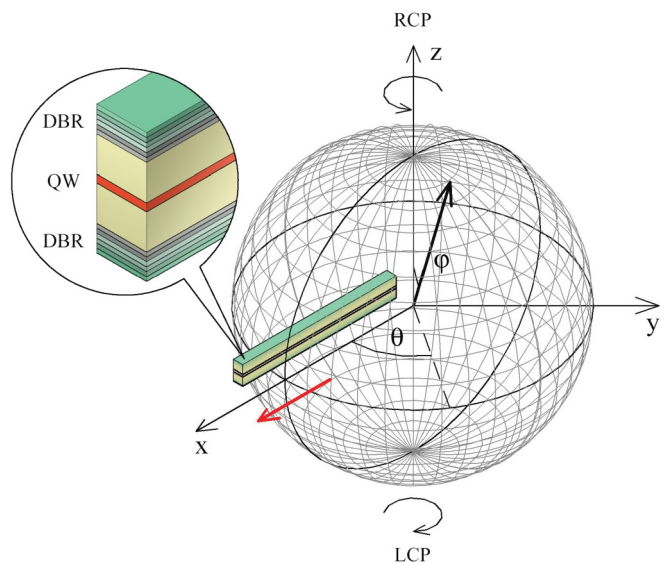


FIG. 1. (Color online) Sketch of the system showing the position of the polariton channel with respect to the Poincaré sphere (also known as the Bloch sphere and pseudospin sphere). The latter serves to illustrate different possible polarizations of the light. If the vector of the pseudospin lies in the xy plane, then the light is linearly polarized, and if it is parallel to the z axes, then it is circularly polarized. Other orientations correspond to the general case of elliptical polarization. The red arrow shows the direction of the effective magnetic field created by the longitudinal-transverse splitting $\mathbf{\Omega}$.

of the laser mode. The system keeps staying at this high-populated state with further increase of the pump intensity. In the backward direction, when we decrease the intensity of the pump, the bistable transition to the low-populated state appears at the lower pump intensity ($P_{th}^{(\leftarrow)} < P_{th}^{(\rightarrow)}$) and a hysteresis curve appears.

Accounting for spin, the polariton-polariton interaction becomes polarization dependent, which leads to multistability of the polariton circular polarization (see Ref. 37 for a detailed discussion of the situation at $T = 0$). This effect is illustrated in the main plot of Fig. 2 for different temperatures, where the pump intensity is fixed and its circular polarization degree \wp_p is being changed. Let us explain this phenomenon with the help of the above discussion for the spinless case. Keeping the total pump intensity, let us change its circular polarization from σ^- ($\phi = \pi$, and $\wp_p = -1$) to σ^+ ($\phi = 0$, and $\wp_p = 1$); see Fig. 1. Initially, there exists only σ^- polaritons in the ground state, thus $\wp_c = -1$. As \wp_p is increased, the σ^+ component starts to become more populated, and at a certain threshold value of \wp_p , the first bistable jump up in \wp_c occurs that implies the abrupt increase of the σ^+ component. A further increase of \wp_p leads to the second jump up of the polarization degree \wp_c due to the bistability jump down of the σ^- component from a high-population state to a low-population state. Finally, the system reaches the state with only the σ^+ component and $\wp_c = 1$. In the backward direction (decrease pump polarization degree from $+1$ to -1), the first jump down is due to the abrupt increase of the σ^- component, while the second jump down is explained by the abrupt decrease of the σ^+ component occupancy.

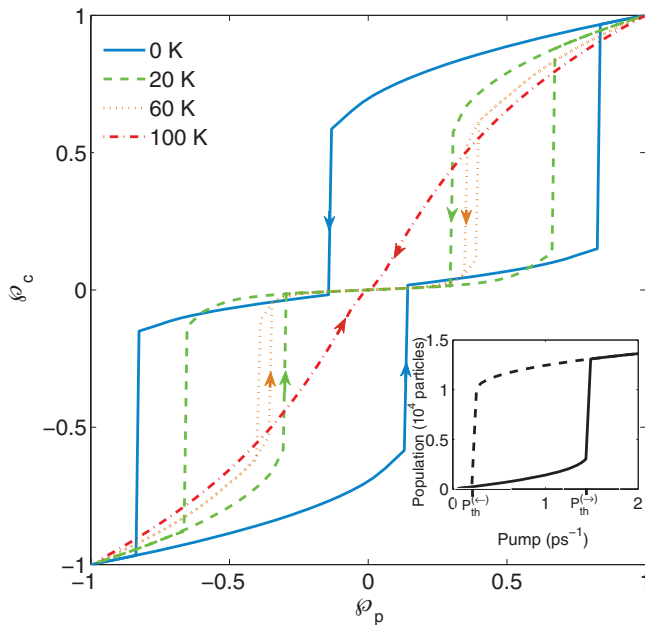


FIG. 2. (Color online) Dependence of the circular polarization degree of the driven polariton mode on the circular polarization degree of the driving pump in the absence of TE-TM splitting for different temperatures. Hysteresis loops, the signatures of the multistability behavior, shrink with the increase of temperature ($T = 0, 20, 60$ K) and finally disappear at $T \approx 100$ K. Inset: dependence of polariton population vs pumping intensity for a single-component system demonstrating the phenomenon of bistability ($T = 0$ K).

With increasing temperature, the multistability loops start to shrink and become totally destroyed at about $T \approx 100$ K. It occurs due to the dissipation processes coming from the interaction with acoustic phonons. At higher temperature, the spin-independent polariton-phonon interaction makes the dependence $\varphi_c(\varphi_p)$ quasilinear, as should be expected; indeed, in the case when coherent nonlinearities play no role and there is no transition between circular polarized components, the polarization degree of the system should coincide with those of the pump.

Now let us introduce the TE-TM splitting to see its effect on polarization multistability. The corresponding term removes the isotropy in the xy plane since it acts as an effective magnetic field in the $+x$ direction. Consequently, the population of each component $n_{\mathbf{k}}^{\pm}$ becomes dependent not only on circular polarization of the pump, by also on the in-plane components of its pseudospin, as can be seen from Eq. (22). In Fig. 3, the dependence of the internal circular polarization degree of the system φ_c is plotted as a function of the circular polarization degree of the pump φ_p for three different in-plane angles θ between the in-plane pseudospin of the pump and the direction along the wire: axis Ox (see Fig. 1). Azimuthal angle θ comes in the pumping Hamiltonian as the relative phase factor between the pumping amplitudes, i.e., $p_+ = e^{i\theta} p_-$. It is observed that the relative phase drastically modifies the profile of the $\varphi_c(\varphi_p)$ plot. First, we note that a finite y component of the pump pseudospin ($\theta \neq 0, \pi$) destroys the symmetry of the multistability curve with respect to the change of the sign of circular polarization of the pump (see dotted green line). Also,

comparing the results for $\theta = 0$ ($+x$ direction) and $\theta = \pi$ ($-x$ direction) cases, we see two quite different polarization behaviors. This difference can be understood from the first term of the kinetic equation (23) for S_{\perp} , where the two cases ($\theta = 0$ and $\theta = \pi$) give contributions with opposite signs. Therefore, the internal circular polarization degree becomes highly sensitive to the choice of meridian on the surface of the Poincaré sphere along which the circular polarization of the laser is changed between σ^+ and σ^- . It should be noted that for a circularly polarized pump, the effect of rotation of the pseudospin due to TE-TM splitting is invisible: for the used value $\Omega = 0.08$ meV and circular polarized pump, the effect of macroscopic self-trapping plays a major role^{6,42–44} and the rotation of pseudospin is blocked. For reduced values of circular polarization, the self-trapping regime is lost and the effects of TE-TM splitting become visible.

Let us, finally, analyze the combined effect of the TE-TM splitting and scattering on phonons (in the rest of the calculations, the in-plane component of the pump pseudospin is taken along the $+x$ direction, i.e., $\theta = 0$). As was shown before in Fig. 2, in the absence of TE-TM splitting, due to the dissipative nature of polariton-phonon interactions the hysteresis behavior is washed out at 100 K. On the other hand, if $\Omega \neq 0$, as in Fig. 4, then the bistable behavior can be recovered and bistability phenomena can survive up to higher temperatures as compare to the case $\Omega = 0$. However, instead of the two-stepped hysteresis loop shown in Fig. 3, we observe only one-stepped behavior. This result suggests the transition from two-independent modes dynamics (the two modes are

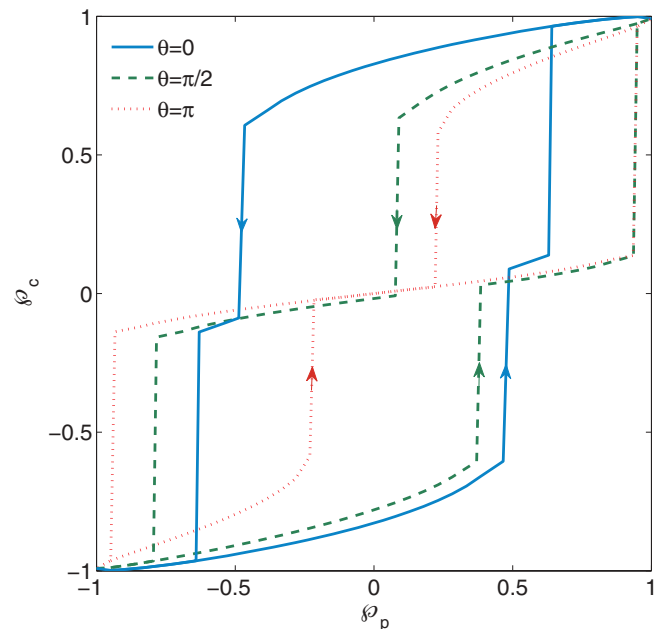


FIG. 3. (Color online) Internal vs external circular polarization degree for different xy -plane projections of the pseudospin of the pump (different azimuthal angles θ) for $\Omega = 0.08$ meV, and $T = 0$ K. Due to the finite value of the TE-TM coupling, the equivalency between the x and y linear polarizations is broken. Therefore, the choice of meridian line of the Poincaré sphere along which the pump laser evolves from the σ^- to σ^+ state becomes crucial for the polarization dynamics of the polariton system.

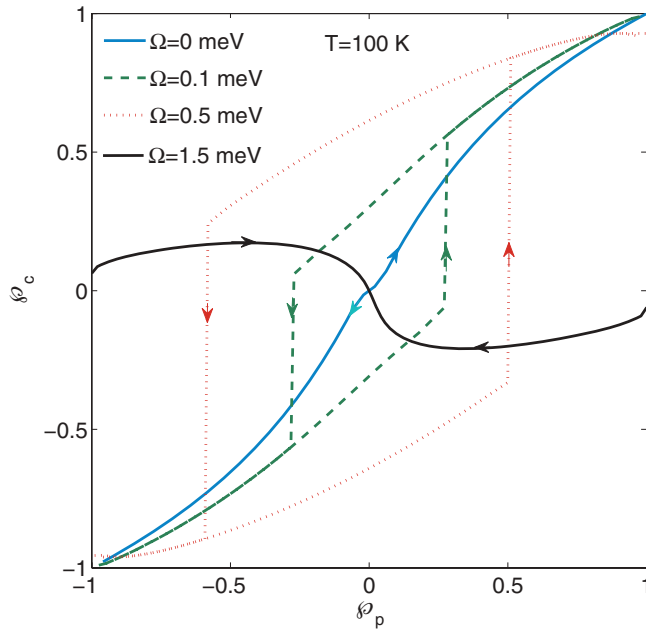


FIG. 4. (Color online) Circular polarization degree of the driven mode vs the circular polarization degree of pump for different values of the longitudinal-transverse splitting Ω for $T = 100$ K. Thus, TE-TM splitting revives the bistability behavior even at high temperature values. At strong TE-TM splittings, i.e., $\Omega = 1.5$ meV, the circular polarizability diminishes due to strong mixing of the σ^\pm modes, and the hysteresis loop disappears.

the mode with σ^+ and the mode with σ^- polarizations) to a single collective mode dynamics. In fact, at some critical value of the TE-TM splitting (around 0.1 meV in our parameter regime), the transition from a high-population state to a low-population state of the one mode is always accompanied by the simultaneous transition from a low-population state to a high-population state of the other mode, and crossover from the multistable behavior to the bistable occurs.

If one increases the value of the TE-TM splitting field even further, polaritons would prefer to stay in a quasilinearly polarized state due to strong mixing of the σ^\pm modes, even for pumping by the fully circularly polarized laser. This situation occurs at $\Omega = 1.5$ meV in Fig. 4, where polaritons become highly linearly polarized even at the values of $\phi_p = \pm 1$ due to the high value of the effective magnetic field in the $+x$ direction. The last term in Eq. (23) is responsible for this behavior. The particles align their pseudospin parallel to the strong effective magnetic field to minimize the total energy in the system. Meanwhile, the hysteresis behavior vanishes, and the difference between the backward and forward swappings disappears.

IV. CONCLUSIONS

In conclusion, we developed a formalism for the description of the dissipative dynamics of an inhomogeneous spinor polariton system in real space and time, accounting for polariton-polariton interactions, polariton-phonon scattering, and effect of the TE-TM effective magnetic field. We applied our formalism to a one-dimensional polariton condensate at different temperatures to investigate the dynamics of the circular polarization of the system when it is driven by the external homogeneous laser pump. We showed that the polarization of the condensate is highly sensitive, not only to the history of the strength of the pump, but also to the phase of the elliptical polarization degree of this pump. In the presence of a TE-TM field, we observe the survival of this phenomena up to very high temperatures.

ACKNOWLEDGMENTS

We thank E. B. Magnusson for useful discussions and help with numerical calculations. The work was supported by Rannis ‘‘Center of Excellence in Polaritonics’’ and FP7 IRSES project ‘‘SPINMET.’’ I.G.S. and I.A.S. thank the International Institute of Physics for their hospitality.

- ¹J. Kasprzak, M. Richard, S. Kundermann, A. Baas, P. Jeambrun, J. M. J. Keeling, F. M. Marchetti, M. H. Szymanska, R. Andre, J. L. Staehli, V. Savona, P. B. Littlewood, B. Deveaud, and Le Si Dang, *Nature (London)* **443**, 409 (2006).
- ²S. Christopoulos, G. Baldassarri Höger von Högersthal, A. Grundy, P. G. Lagoudakis, A. V. Kavokin, J. J. Baumberg, G. Christmann, R. Butte, E. Feltn, J.-F. Carlin, and N. Grandjean, *Phys. Rev. Lett.* **98**, 126405 (2007).
- ³A. Amo, D. Sanvitto, F. P. Laussy, D. Ballarini, E. del Valle, M. D. Martin, A. Lemaitre, J. Bloch, D. N. Krizhanovskii, M. S. Skolnick, C. Tejedor, and L. Vina, *Nature (London)* **457**, 291 (2009).
- ⁴K. G. Lagoudakis, B. Pietka, M. Wouters, R. Andre, and B. Deveaud-Pledran, *Phys. Rev. Lett.* **105**, 120403 (2010).
- ⁵K. G. Lagoudakis, T. Ostatnicky, A. V. Kavokin, Y. G. Rubo, R. Andre, and B. Deveaud-Pledran, *Science* **13**, 974 (2009).
- ⁶I. A. Shelykh, D. D. Solnyshkov, G. Pavlovic, and G. Malpuech, *Phys. Rev. B* **78**, 041302 (2008).
- ⁷F. P. Laussy, A. V. Kavokin, and I. A. Shelykh, *Phys. Rev. Lett.* **104**, 106402 (2010).

- ⁸For a recent review on polariton devices, see T. C. H. Liew, I. A. Shelykh, and G. Malpuech, *Physica E* **43**, 1543 (2011).
- ⁹A. Imamoglu and J. R. Ram, *Phys. Lett. A* **214**, 193 (1996).
- ¹⁰I. A. Shelykh, K. V. Kavokin, A. V. Kavokin, G. Malpuech, P. Bigenwald, H. Deng, G. Weihs, and Y. Yamamoto, *Phys. Rev. B* **70**, 035320 (2004).
- ¹¹E. Wertz, L. Ferrier, D. Solnyshkov, R. Johne, D. Sanvitto, A. Lemaitre, I. Sagnes, R. Grousson, A. V. Kavokin, P. Senellart, G. Malpuech, and J. Bloch, *Nature Phys.* **6**, 860 (2010).
- ¹²T. C. H. Liew, A. V. Kavokin, and I. A. Shelykh, *Phys. Rev. Lett.* **101**, 016402 (2008).
- ¹³T. C. H. Liew, A. V. Kavokin, T. Ostatnicky, M. Kaliteevski, I. A. Shelykh, and R. A. Abram, *Phys. Rev. B* **82**, 033302 (2010).
- ¹⁴A. T. Hammack, M. Griswold, L. V. Butov, L. E. Smallwood, A. L. Ivanov, and A. C. Gossard, *Phys. Rev. Lett.* **96**, 227402 (2006); R. B. Balili, D. W. Snoke, L. Pfeiffer, and K. West, *Appl. Phys. Lett.* **88**, 031110 (2006); O. El Daif, A. Baas, T. Guillet, J.-P. Brantut, R. Idrissi Kaitouni, J. L. Staehli, F. Morier-Genoud, and B. Deveaud, *ibid.* **88**, 061105 (2006); R. I. Kaitouni, O. El

- Daif, A. Baas, M. Richard, T. Paraiso, P. Lugan, T. Guillet, F. Morier-Genoud, J. D. Ganiere, J. L. Staehli, V. Savona, and B. Deveaud, *Phys. Rev. B* **74**, 155311 (2006); M. M. Kaliteevskii, S. Brand, R. Abram, I. Iorsh, A. Kavokin, and I. Shelykh, *Appl. Phys. Lett.* **95**, 251108 (2009).
- ¹⁵A. V. Kavokin, G. Malpuech, and M. Glazov, *Phys. Rev. Lett.* **95**, 136601 (2005).
- ¹⁶M. M. Glazov and L. E. Golub, *Phys. Rev. B* **77**, 165341 (2008).
- ¹⁷I. A. Shelykh, G. Pavlovic, D. D. Solnyshkov, and G. Malpuech, *Phys. Rev. Lett.* **102**, 046407 (2009).
- ¹⁸I. A. Shelykh, Yuri G. Rubo, G. Malpuech, D. D. Solnyshkov, and A. Kavokin, *Phys. Rev. Lett.* **97**, 066402 (2006).
- ¹⁹M. Wouters and I. Carusotto, *Phys. Rev. Lett.* **99**, 140402 (2007).
- ²⁰M. O. Borgh, J. Keeling, and N. G. Berloff, *Phys. Rev. B* **81**, 235302 (2010).
- ²¹M. Wouters, T. C. H. Liew, and V. Savona, *Phys. Rev. B* **82**, 245315 (2010).
- ²²C. Piermarocchi, F. Tassone, V. Savona, A. Quattropani, and P. Schwendimann, *Phys. Rev. B* **53**, 15834 (1996).
- ²³F. Tassone and Y. Yamamoto, *Phys. Rev. B* **59**, 10830 (1999).
- ²⁴D. Sarchi and V. Savona, *Phys. Rev. B* **75**, 115326 (2007).
- ²⁵F. P. Laussy, G. Malpuech, A. Kavokin, and P. Bigenwald, *Phys. Rev. Lett.* **93**, 016402 (2004).
- ²⁶D. M. Whittaker and P. R. Eastham, *Europhys. Lett.* **87**, 27002 (2009).
- ²⁷D. Porras, C. Ciuti, J. J. Baumberg, and C. Tejedor, *Phys. Rev. B* **66**, 085304 (2002).
- ²⁸J. Kasprzak, D. D. Solnyshkov, R. Andre, Le Si Dang, and G. Malpuech, *Phys. Rev. Lett.* **101**, 146404 (2008).
- ²⁹T. D. Doan, H. T. Cao, D. B. Tran Thoai, and H. Haug, *Phys. Rev. B* **72**, 085301 (2005).
- ³⁰H. T. Cao, T. D. Doan, D. B. Tran Thoai, and H. Haug, *Phys. Rev. B* **77**, 075320 (2008).
- ³¹I. G. Savenko, E. B. Magnusson, and I. A. Shelykh, *Phys. Rev. B* **83**, 165316 (2011).
- ³²E. B. Magnusson, I. G. Savenko, and I. A. Shelykh, *Phys. Rev. B* **84**, 195308 (2011).
- ³³H. Carmichael, *Quantum Optics I: Master Equations And Fokker-Planck Equations* (Springer, New York, 2007).
- ³⁴A. Kavokin and G. Malpuech, *Cavity Polaritons* (Elsevier, Amsterdam, 2003).
- ³⁵K. V. Kavokin, I. A. Shelykh, A. V. Kavokin, G. Malpuech, and P. Bigenwald, *Phys. Rev. Lett.* **92**, 017401 (2004).
- ³⁶I. A. Shelykh, A. V. Kavokin, Yu. Rubo, T. C. H. Liew, and G. Malpuech, *Semicond. Sci. Technol.* **25**, 013001 (2010).
- ³⁷N. A. Gippius, I. A. Shelykh, D. D. Solnyshkov, S. S. Gavrilov, Yuri G. Rubo, A. V. Kavokin, S. G. Tikhodeev, and G. Malpuech, *Phys. Rev. Lett.* **98**, 236401 (2007).
- ³⁸A. Baas, J.-Ph. Karr, M. Romanelli, A. Bramati, and E. Giacobino, *Phys. Rev. B* **70**, 161307 (2004).
- ³⁹T. K. Paraiso, M. Wouters, Y. Leger, F. Morier-Genoud, and B. Deveaud-Pledran, *Nature Mater.* **9**, 655 (2010).
- ⁴⁰A. Amo, T. C. H. Liew, C. Adrados, R. Houdre, E. Giacobino, A. V. Kavokin, and A. Bramati, *Nature Photon.* **4**, 361 (2010).
- ⁴¹I. A. Shelykh, A. V. Kavokin, and G. Malpuech, *Phys. Status Solidi B* **242**, 2271 (2005).
- ⁴²A. Smerzi, S. Fantoni, S. Giovanazzi, and S. R. Shenoy, *Phys. Rev. Lett.* **79**, 4950 (1997).
- ⁴³G. J. Milburn, J. Corney, E. M. Wright, and D. F. Walls, *Phys. Rev. A* **55**, 4318 (1997).
- ⁴⁴S. Raghavan, A. Smerzi, S. Fantoni, and S. R. Shenoy, *Phys. Rev. A* **59**, 620 (1999).